

A New Biomarker for Mitotic Cells

James W. Jacobberger,^{1*} Phyllis S. Frisa,¹ R. Michael Sramkoski,¹ Tammy Stefan,¹
Keith E. Shults,² Deena V. Soni³

¹Case Comprehensive Cancer Center,
Case Western Reserve University,
Cleveland, Ohio 44106

²Esoterix Center for Innovation, 201
Summit View Drive, Brentwood,
Tennessee 37027

³Department of Environmental Health,
Case Western Reserve University,
Cleveland, Ohio 44106

Received 21 August 2007; Accepted
7 November 2007

This article contains supplementary
material available via the Internet at
[http://www.interscience.wiley.com/
pages/1552-4922/suppmat](http://www.interscience.wiley.com/pages/1552-4922/suppmat).

Grant sponsor: PHS; Grant number: R01-
CA473413; Grant sponsor: National
Cancer Institute; Grant number: P30-
CA43703; Grant sponsor: Advanced
Technology Center, Beckman Coulter,
Inc.

Present address of Deena V. Soni:
Department of Molecular Pharmacology,
Stanford University, Palo Alto, CA.

*Correspondence to: James W.
Jacobberger, Case Comprehensive
Cancer Center, Case Western Reserve
University, Cleveland, OH 44106, USA.

Email: jwj@case.edu

Published online 4 December 2007 in
Wiley InterScience ([www.interscience.
wiley.com](http://www.interscience.wiley.com))

DOI: 10.1002/cyto.a.20501

© 2007 International Society for
Analytical Cytology

• Abstract

Many epitopes are phosphorylated during mitosis. These epitopes are useful biomarkers for mitotic cells. The most commonly used are MPM-2 and serine 10 of histone H3. Here we investigated the use of an antibody generated against a phospho peptide matching residues 774–788 of the human retinoblastoma protein 1 (Rb) to detect mitotic cells. Human cell lines were stained with DNA dyes and antibodies reactive with epitopes defined by antibody MPM-2, phospho-S10-histone-H3, and the phospho-serine peptide, TRPPTLSPIPHIPRC (phospho-S780-Rb). Immunoreactivity and DNA content were measured by flow and image cytometry. Correlation and pattern recognition analyses were performed on list mode data. Western blots and immunoprecipitation were used to investigate the number of peptides reactive with phospho-S780-Rb and the relationship between reactivity with this antibody and MPM-2. Costaining for bromodeoxyuridine (BrdU) was used to determine acid resistance of the phospho-S780-Rb epitope. Cell cycle related phospho-S780-Rb immunofluorescence correlated strongly with that of MPM-2. Laser scanning cytometry showed that phospho-S780-Rb immunofluorescence is expressed at high levels on all stages of mitotic cells. Western blotting and immunoprecipitation showed that the epitope is expressed on several peptides including Rb protein. Costaining of BrdU showed that the epitope is stable to acid. Kinetic experiments showed utility in complex cell cycle analysis aimed at measuring cell cycle transition state timing. The phospho-S780-Rb epitope is a robust marker of mitosis that allows cytometric detection of mitotic cells beginning with chromatin condensation and ending after cytokinesis. Costaining of cells with DNA dyes allows discrimination and counting of mitotic cells and post-cytokinetic (“newborn”) cells. To facilitate use without confusion about specificity, we suggest the trivial name, pS780 for this mitotic epitope. © 2007 International Society for Analytical Cytology

• Key terms

cell cycle analysis; flow cytometry; image cytometry; immunofluorescence; retinoblastoma protein; phosphorylation; mitosis

CYTOMETRIC analysis of the cell cycle that includes mitosis has been reported intermittently for many years (see references in 1,2). The most straightforward assays use immunofluorescence of mitotic epitopes combined with DNA content. These epitopes are on single proteins (2,3), reside on multiple proteins (1,4), are degraded in mitosis (2,5), or unmasked during mitosis (6). Although advantages of objectivity, ability to count large numbers of events, and ability to correlate measurements are obvious reasons to use flow or laser scanning cytometry (LSC) to count mitotic cells, the approach has been used infrequently until recently. Now, it is more common to see the use of cytometry to quantify mitotic cells in studies that are biological and not methodological in theme. This may be due to the wide commercial availability of primary conjugates of MPM-2 and phospho-S10-histone H3 antibodies.

An area of cytometry that has seen recent increased interest is the correlated measurement of biochemical activities, especially phosphorylation (7–9). In this work, the central theme, sometimes more implicit than explicit, has been analysis of pathways and networks rather than assays of single activities. Perhaps for the first

time, this approach employs cytometry mainly for quantitative correlation and analysis of complexity rather than the more often cited reasons of convenience and objectivity. For analysis of biochemical networks, cytometry is perhaps the most powerful approach available when the questions are directed and limited to ~20 variables or less. This is because of correlation, precise quantification, and ability to examine all possible states¹ within a single or limited number of samples.

Although most emphasis on biochemical networks within the cytometry community is on signaling pathways, the cell cycle is a biochemical network and highly multiparametric approaches to cell cycle analyses can be equally compelling. Indeed, any regulatory pathway can be analyzed by cytometry with powerful results (e.g., 10). The reason for this is that biochemical networks cannot be conceived except dynamically, and cell populations exist in all possible biochemical states with respect to time for a given environment. This is especially easy to see for asynchronous populations of cycling cells in which all biochemical states are extant at any given time. Analysis of the “regulatory” cell cycle within this context is more easily digested when layered on a backbone of phases and stages that we “understand” from kinetics and morphology. In this sense, the backbone cytometry assay is DNA content coupled with a mitotic marker and at least for the late phases (S, G₂, and M), cyclins A2 and B1 for somatic cells. For each of these backbone markers, it is good to have alternative markers. For mitosis, there are two reasons not to be satisfied with phospho-S10-histone H3 and MPM-2 as the only cytometric mitotic markers. First, in studies of drug inhibitions and interactions, phospho-S10-histone H3 phosphorylation in mitosis is governed by aurora kinase B (11–13), and therefore, any treatment that results in reduced aurora kinase B activity, may result in a compromised or eliminated backbone. MPM-2 is a good alternative in this case because the epitope is expressed on many proteins and phosphorylated by several enzymes (14,15). Therefore, in studies in which enzyme activity is depleted, the epitope may not be so depleted so as to render the backbone unusable.² Second, in multivariate studies matching fluorescence colors to epitopes in terms of fluorophore characteristics (wavelength, extinction coefficient, and quantum yield) and antigen abundance is a continuous challenge (for a discussion of similar problems on surface immunophenotype, see 17). While many phosphorylated epitopes, which turn out to be the best mitotic markers, are abundant in mitosis, the commercial availability of only two fluorochromes is limiting. Therefore, it would be valuable to have additional antibodies to robust markers available in forms that can be integrated in assays of several mouse monoclonal antibodies. The serine at residue 780 of Rb is a specific substrate

¹Here, a biochemical state of the cell is defined as the conjunction of biochemical activities that are extant for a long enough period of time for asynchronous cells to “cluster” at those measurements.

²Indeed, we can knock down cyclin B1 and reduce cyclin B1/Cdk1 kinase activity by 99% and reduce MPM-2 reactivity by only 30% (unpublished results) but the cytometric pattern for DNA versus a mitotic marker remains intact. This robustness has been argued previously as a positive factor for MPM-2 as a marker for mitosis (16).

of cyclin D/Cdk4 (18,19) and not Cdk2. We discovered by accident that antibody raised to the phospho-peptide, RPPTLS⁷⁸⁰PIPHIPR stains mitotic cells intensely. Here, we show that the epitope, defined by this antibody is a robust mitotic marker that is equivalent to MPM-2.

MATERIALS AND METHODS

Cells and Cell Culture

The culture and sources of human cell lines: DU-145, PC3, LNCaP, and 22Rv1 (prostate cancer); Molt4 and K562 (T cell lymphoma and chronic myelogenous leukemia), and HeLa (cervical carcinoma) are conventional and have been published (20–22). hTert-RPE-1 cells (Clontech; Mountain View, CA) were cultured in DMEM/F-12 with 2 mM L-glutamine, 0.375% sodium bicarbonate, 50 µg/ml gentamicin sulfate, and 10% fetal bovine serum (FBS) (Cambrex, Charles City, IA). SAOS-2 cells were grown in McCoy’s modified media with 15% FBS and gentamicin sulfate. Media and additives were from Thermo Fisher Scientific (Waltham, MA) and Gibco (Carlsbad, CA).

Culture for Laser Scanning Confocal Microscopy and Cytometry

hTert-RPE-1 cells (30,000) were applied in 100 µl of culture medium to the microwell of collagen (rat tail type I, Sigma-Aldrich, St. Louis, MO) coated 35 mm glass bottom microwell dishes (MatTek, Ashland, MA). An additional 2 ml of culture medium was added after 30 min, and the cells were incubated at 37°C in a humidified 5% CO₂ atmosphere for 48 h.

Inhibitors

Okadaic acid (OA) and nocodazole were obtained from Sigma-Aldrich (St. Louis, MO).

Antibodies

Antibodies were obtained and used per 1–2 × 10⁶ cells as follows: 0.125 µg MPM-2 and MPM-2-FSE (FSE = fluorescein-5-EX succinimidyl ester; Millipore/Upstate Biotechnologies, Lake Placid, NY); 0.125–0.5 µg Alexa Fluor 488 or 647 conjugated phospho-S10-histone H3 (Millipore/Upstate Biotechnologies); Rb (BD Biosciences, San Jose, CA; clone G3-245; cat 554136); 0.5–1.0 µl phospho-S780-Rb (Cell Signaling Technology, Danvers, MA); 0.5 µg Alexa Fluor 647 conjugated anti-BrdU (A647-BrdU, Phoenix Flow Systems, San Diego, CA); 1 µg of phycoerythrin (PE) conjugated anti-cyclin A (Beckman Coulter, Miami, FL). Secondary antibodies were used at 2:1 ratio w/w and obtained from Molecular Probes-Invitrogen (Carlsbad, CA). The conjugated fluorochromes varied and are denoted in Figure legends. All staining reactions were carried out in 50 µl volumes of PBS with 2% BSA.

DNA Dyes

DAPI or Hoechst 33342 (Molecular Probes, Invitrogen) were used at 1 µg per 10⁶ cells. 7-Amino actinomycin D (7-AAD, Molecular Probes, Invitrogen) was used at 25 µg/ml. For 7-AAD staining, cells were incubated with 10,000 Kunitz units Rnase (Worthington Biochemical, Lakewood, NJ).

Fixation

Preparation of attached cells as single cells suspensions was by trypsinization and has been described in detail (23). Fixation was with 90% methanol or a low concentration of formaldehyde followed by 90% methanol and has been described in detail (24). Hematopoietic cells are fixed directly by addition of a low concentration of formaldehyde to the culture medium followed by washing and fixation/denaturation with 90% methanol (21).

Flow Cytometry Staining

This has been described in detail (21–26).

Staining for Laser Scanning Confocal Microscopy and Cytometry

The cells were fixed on the plate with 0.125% formaldehyde added directly to the culture medium for 10 min at 37°C followed by cold 90% MeOH in PBS. Antibody staining was carried out as for flow cytometry except that the reaction volume was 100 μ l. DNA was stained with 0.5 μ g/ml DAPI in PBS with 1% glycerol (v/v) and 2% *n*-propyl gallate (w/v).

Kinetic Experiments

Molt4 were pulsed with 20 μ M BrdU (Sigma-Aldrich) then chased with 100 μ M thymidine (Sigma-Aldrich), sampled periodically, fixed with 0.125% formaldehyde/90% methanol (24) then processed for BrdU staining as described (22) with the following changes: all staining and washes were done at 4°C and all staining and wash solutions (PBS with 2% BSA) contained 0.5% Triton X-100 except the final running solution.

Flow Cytometry

Flow cytometry was performed on BD Biosciences LSR I, LSR II, and Beckman Coulter XL, and FC-500 instruments set up with stock filters supplied by the manufacturers.

Laser Scanning Cytometry

LSC was performed with a Compucyte (Cambridge, MA) iCye using violet and red lasers to excite DAPI and Alexa 647 fluorochromes, respectively. Stock filters from the manufacturer were used and the contouring algorithm relied on a composite gray scale image using the Max function for two input images (DAPI and phospho-S780-Rb). This had the advantage that anaphase through cytokinetic cells were contoured as a single event rather than two (as would happen if the nuclear image alone were used).

Confocal Microscopy

Cells were imaged with a Zeiss LSM 510 inverted laser-scanning confocal fluorescence microscope using 63X (NA = 1.4) oil planochromat objective (Carl Zeiss, Thornwood, NY). Each image was obtained by independent laser scanning. Laser excitations were at 325, 488, and 633 nm. Images were written in TIF format with supplied software. Composite images were produced with Adobe Photoshop CS2 (Adobe Systems, San Jose, CA).

SDS-PAGE and Western blotting

SDS-PAGE and immunoblotting techniques were conventional and have been reported in detail (27). Cell lysates contained phosphatase inhibitors (5 mM sodium orthovanadate and 5 mM sodium fluoride in addition to protease inhibitors). Blots were visualized with alkaline phosphatase conjugated rabbit or mouse secondary antibody (Promega, Madison, WI) using chemiluminescent detection with CDP-Star substrate (Tropix, Bedford, MA). Images were developed on X-ray film or the FluorS Imager (Biorad, Hercules, CA). Quantification was performed using Quantity One 4.1.1 software (Bio-Rad).

Phosphatase Treatment

Western blots were divided in two and treated with calf intestinal mucosa alkaline phosphatase (CAP, New England Biolabs, Ipswich, MA) or buffer alone before immunostaining with phospho-S780-antibody. CAP was 500 U/ml in buffer containing 100 mM NaCl, 50 mM Tris-HCl, 10 mM MgCl₂, and 1 mM dithiothreitol at pH 7.9 (manufacturer's formula). After 30 min incubation at room temperature the membrane was washed three times in Tris buffered saline with 0.1% Tween 20, pH 8.0, dried, and soaked in methanol for 5 min to inactivate the CAP. The membrane was rehydrated and processed as above.

Immunoprecipitation

Cells were lysed in nondenaturing lysis buffer (50 mM Tris, 150 mM NaCl, 5 mM dithiothreitol, 1% NP40, pH 7.4 with protease and phosphatase inhibitors). The lysate (500 μ g protein) was cleared by nutating with 2 μ g rabbit IgG and 50 μ l of protein A agarose beads (Sigma-Aldrich) for 1 h then centrifuging and removing and saving the supernatant. A 1:100 dilution of the phospho-S780-Rb antibody was added to the supernatant, nutated for 2.5 h and then 50 μ l Protein A agarose beads were added and nutated over night. The washed pellet was dissolved in SDS sample buffer by heating, with a final SDS concentration of 4.4%.

Analysis

Data processing, display, gating, and region setting were performed with WinList 6.0 (Verity Software House, Topsham, ME). Pattern recognition was by eye and experience. Regions were set on clusters using boxes, ovals, or amorphous containers or on contour levels. For kinetic analysis, data were fit with nonlinear least square methods (GraphPad Prism 5.00, GraphPad Software, San Diego, CA, www.graphpad.com). The "percentage of labeled cells" data versus time were fit with sigmoid dose response functions. Except for the data from the regions labeled R6/R6b and R12/R12b (see Fig. 9), the bottom and top parameters were set to 0 and 100. For the R6/R6b data, the bottom was set to the labeling index (54) to account for contamination of S phase cells and movement of the label during the 30 min of labeling time. For the R12/R12b data, a five parameter function was used to obtain an adequate fit. This is likely due to contamination of true positive cells with negative cells.

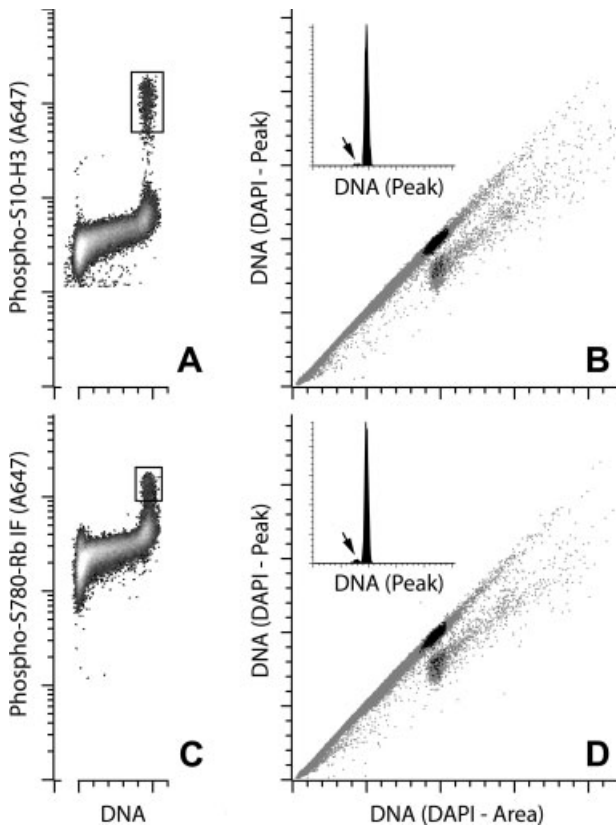


Figure 1. Mitotic patterns: Molt4 cells were fixed and stained for the mitotic marker, phospho-S10-histone H3 (phospho-S10-H3), or with antibody phospho-S780-Rb followed with Alexa 647 (A647) conjugated secondary and DAPI. IF = immunofluorescence. **A** and **C**: gated singlet 2C population with regions set on mitotic cells (boxes). **B** and **D**: doublet discrimination (ungated events) with mitotic cells color coded black (gated from regions set in A and C). Some late mitotic cells [telophase and cytokinetic cells that have not separated can register as doublets if the cytometer is aligned well enough and the beam is narrow enough (39)]. Insets: Peak DNA signal histograms of mitotic cells; telophase and cytokinetic clusters are denoted by arrows.

RESULTS AND DISCUSSION

Bivariate Analysis Shows that Reactivity with the Phospho-S780-Rb Antibody Marks Mitosis

Because serine 780 of Rb is a substrate for Cdk4 (18,19), we first stained cells with phospho-S780-Rb in a search for epitopes that might prove interesting for analysis of the G1 phase of the cell cycle. To our surprise, analysis of correlated cytometric data for DNA and immunofluorescence was typical for a mitotic marker (Fig. 1). Compared with an established marker, phospho-S10-histone H3 (2), the ratio of the signal of M to G2 was less but the fraction of cells clustering at peak levels was similar (Fig. 1). We costained cells for a second established mitotic marker, MPM-2 (4), and directly demonstrated in Molt4 cells concordance between the phospho-S780-Rb epitope (pS780)³

³To avoid confusion about specificity, from this point, the antibody is referred to as “phospho-S780-Rb” and the epitope will be referred to as “pS780.”

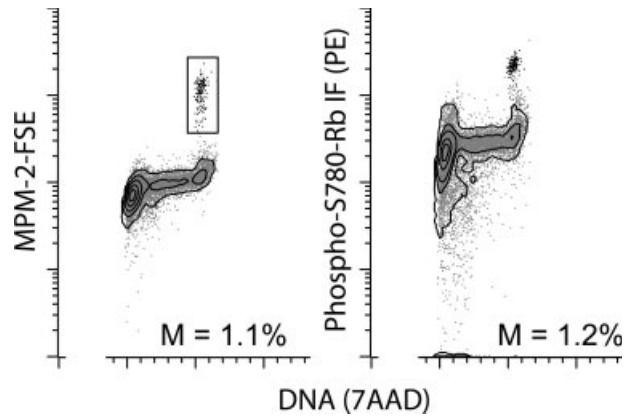


Figure 2. Phospho-S780-Rb and MPM-2 immunofluorescence are coincident. Molt4 cells were fixed and stained with primary conjugated MPM-2 and phospho-S780-Rb as above except a phycoerythrin (PE) conjugated secondary was used in conjunction with 7-AAD for DNA. The singlet 2C stemline was gated by doublet discrimination (not shown). MPM-2 versus DNA displayed a typical mitotic cell cycle pattern. Mitotic cells were gated on MPM-2 reactivity (left panel) and color-coded black. The color coded mitotic cells are mapped to the phospho-S780-Rb IF versus DNA pattern (right panel). The mitotic percentages (M) from each assay are shown.

and MPM-2 epitope (Fig. 2). Therefore, we showed that immunostaining for pS780 marks mitotic cells by direct and indirect methods with two established mitotic markers.

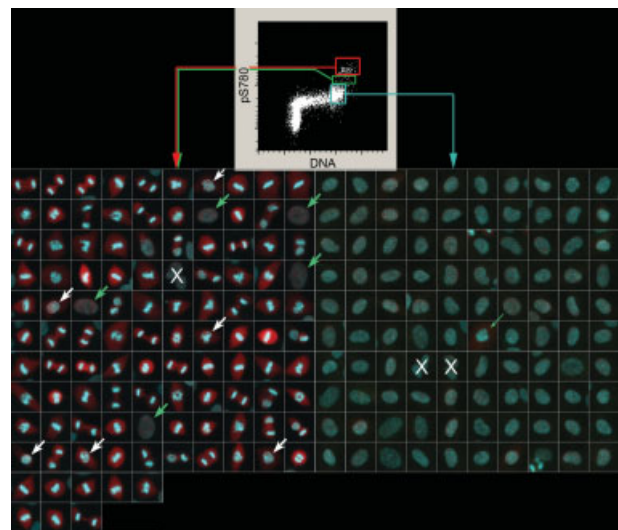


Figure 3. LSC of phospho-S780-Rb immunofluorescence and DNA content. hTert-RPE-1 cells were grown in dishes with coverslip inserts, fixed, then stained for pS780 followed with Alexa 647 secondary and DAPI. Top: immunofluorescence plotted versus DNA content. Images in the left lower panel are composite signals gated from the mitotic cluster (red box) plus the transition region (green box). The lower right panel contains similar images from the G2 gate (cyan box). Left lower panel green arrows: transition cells (4 of 5 localized to green box); white arrows: prophase cells. Lower right panel thin green arrow: prophase cell. X: mistakes in contouring, doublets.

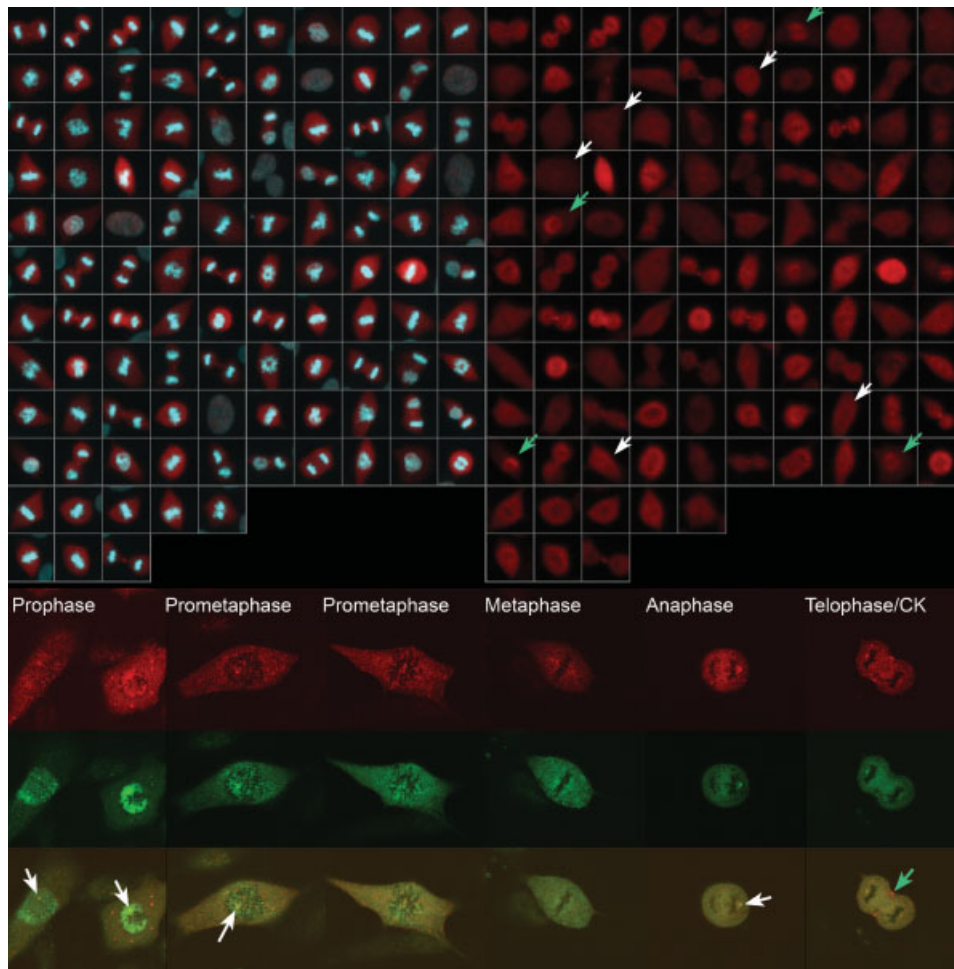


Figure 4. LSC and confocal images of mitotic cells. The cells and experiment are the same as Figure 3. The panel on the top left is the same as in Figure 3 and represents the composite image of all mitotic cells analyzed. The panel on the top right is the pS780 signal only. Green arrows: prophase; white arrows, top right: prometaphase. Lower panel: laser scanning confocal microscopy of hTert-RPE-1 mitotic cells. Red images were obtained by excitation of Alexa 647 secondary for phospho-S780-Rb staining. Green images were obtained by excitation of MPM-2-FSE. The cells were also stained with DAPI for DNA (not shown). Green and red confocal images were processed to reduce the visual impact of low level intensity and increase high level intensity (S shaped input/output curve). This improved S/N and contrast but did not materially change the images. The merged image (bottom row) has not been processed other than merging. Arrows, bottom row: prophase through anaphase—centrosomes; telophase/CK—contractile ring area.

All Mitotic Stages are Positive for pS780 Epitope

Usually, when evaluating the use of a mitotic probe, we have relied on flow cytometry and cell sorting coupled with microscopy to determine whether all the mitotic stages are detected or not (e.g., 25). LSC (28) is perhaps a better approach in that uncertainties of cell preparation of attached cells are eliminated as well as any error in sorting and slide capture. Therefore, we used LSC to ask whether all stages of mitosis were positive for pS780. The results for hTert-RPE-1 cells are shown in Figure 3. hTert-RPE-1 cells are an immortal, euploid, human epithelial cell line (29). In this experiment, the DNA/immunofluorescence bivariate histogram is typical for a mitotic marker and is similar to bivariate flow cytometry data for pS780 (e.g., Figs. 1 and 2). All stages of mitosis are represented. Although in this experiment, late mitotic stages are more prevalent, this was a result of biology rather than technology. All of the mitotic cells on the evaluated coverslip are shown. There

were five cells that had higher than G2 level pS780 fluorescence but G2 nuclear morphology in the larger mitotic region (Fig. 3, red and green regions on histogram; left lower panel, green arrows). These decreased to 1 with the gate set more tightly around the M cluster (red region on histogram, Fig. 3), suggesting that these cells might be classified as either transition cells or early mitotic cells. The white arrows show obvious prophase cells with condensed chromatin and circumscribed nuclei (evidence for intact nuclear membranes). The G2 cells (lower right panel) are randomly representative but all of the G2 cells are not shown. There is one clear and obvious prometaphase cell in this group (right side, thin green arrow). Since, this image shows that the cell is distinctly more red than all the other related cells, the inclusion here is likely to be algorithmic in nature rather than biological. The total number of G2 cells that were evaluated was 150 (100 are shown). Therefore, the false positive rate for mitotic cells should be less than 1% [depending

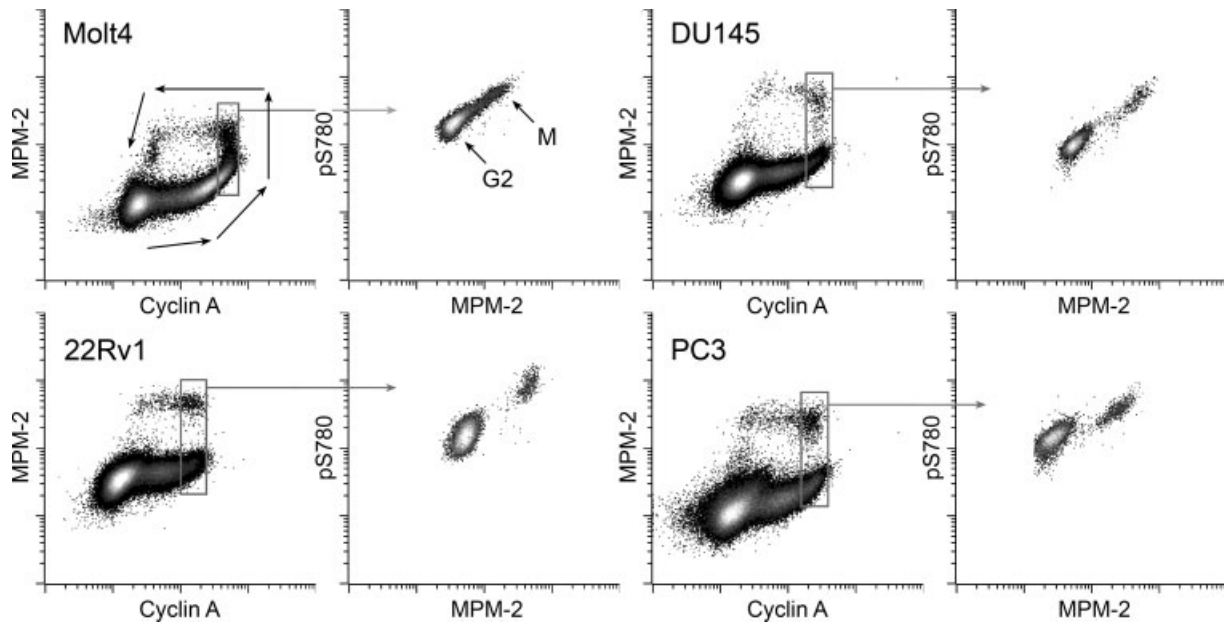


Figure 5. Cyclin A, MPM-2, and pS780 for 4 cell lines. The left hand panel for each named pair shows the cyclin A versus MPM-2 distribution and the right hand panel shows the correlation plots (MPM-2 versus pS780) for only the “late” G2, transition phase, and mitotic cells gated from the left display (gray boxes). Gray arrows indicate that the “pointed to” bivariate plot was gated from the gray boxed region. The black arrows in the Molt4 plot shows the 2D data vector—i.e., the age of the cells increases as a function of position within a distribution about the centroid and orthogonal to the arrows.

on how tightly the region is set and the classification scheme/criteria (i.e., an arbitrary decision on the nature of the transition cells between the G2 and M clusters)]. For G2, the false positive rate is likely to be less than 1%.

The images from LSC suggested that the pS780 fluorescence was predominantly nuclear in prophase (Fig. 4 top right panel, green arrows); uniform in prometaphase (Fig. 4 top right panel, white arrows), and appeared to be reduced or excluded from the chromatin from metaphase onward. To explore this further, we performed confocal microscopy on samples that were prepared identically to those presented in Figure 4 (top panels) except that MPM-2 staining was also performed. Representative cells are shown in Figure 4 (bottom panel). It is clear that both pS780 and MPM-2 staining were excluded or very reduced on the chromatin during all stages. Both pS780 and MPM-2 were nuclear and cytoplasmic during prophase and both become distributed throughout the cell after nuclear envelope breakdown (inferred). Both epitopes are present on centrosomes (Fig. 4 bottom panel, white arrows). MPM-2 dimly lights up the mitotic spindle. The pS780 epitope is expressed strongly on the cleavage furrow (Fig. 4 bottom panel, green arrow; also cytokinetic cells in top right panel). Overall, there is some coincident staining but largely, the green and red signals are separate and not coincident.

Cell Lines that are Deficient for Rb Expression are Efficiently Stained for Mitotic Cells by Phospho-S780-Rb Antibody

The data of Figure 2 suggest that there is a high correlation between expression of the MPM-2 and p-S780-pRb epitopes. The sequence surrounding S780 of Rb (TRPPTLSPI-

PHIPRSC) contains a putative MPM-2 site of XSPXX where the first and fourth amino acids are hydrophobic and the last unchanged or basic (30). To both evaluate the relationship between coexpression of the MPM-2 and pS780 epitopes and the level of contribution of Rb phosphorylation to the staining intensity, we analyzed samples of three human prostate tumor lines, one (DU-145) of which does not express appreciable levels of Rb (31) and compared these to Molt4. The cells were stained for DNA, MPM-2, pS780, and cyclin A. The results are presented in Figure 5. Bivariate plots of cyclin A versus MPM-2 were used to gate G2 and M cells that have the highest levels of cyclin A. These are late G2 and prophase cells, since cyclin A is degraded after nuclear membrane breakdown (32). Gated bivariate plots of MPM-2 versus pS780 were used to make the following observations and calculate Table 1. The following statements can be made.

First, it is clear that in Molt4 cells, there is a high correlation between MPM-2 and pS780 and that result has been observed several times and can be observed visually and by the correlation coefficient for G2+M cells (Table 1).

Second, there is a high but inexact correlation between the two epitopes in each of the prostate cell lines. In each case,

Table 1. Quantitative properties of epitope expression

	RATIO M:G2		CORRELATION		
	MPM-2	pS780	G2	M	G2 + M
22Rv1	9.5	2.7	0.65	0.66	0.89
DU-145	9.2	5.2	0.68	0.69	0.96
PC3	8.4	5.5	0.50	0.51	0.92
Molt4	4.0	2.7	0.68	0.69	0.92

since we know that cyclin A increases in G2 then decreases after prophase, we know the direction of the vector that describes coexpression of cyclin A and MPM-2 through the cell cycle (black arrows in the Molt4 plot). Plots of cyclin A versus pS780 are similar, and the same inference can be drawn. The lack of perfect correlation between the two epitopes during the period of time covering the G2 to M transition⁴ can be accounted for by different rates of expression. The difference in rates appears to occur during the period of G2 to M transition when the epitopes are phosphorylated above the interphase level but not yet to the stable, high mitotic level. During this period of time, for the prostate cell lines, the rate of net phosphorylation of pS780 is less per MPM-2 epitope than it is either before (interphase) or after (prophase). Therefore, if mitotic cells are defined from the first onset of increased phosphorylation, the mitotic count will differ by a small amount dependent on the marker used. These same statements can be made about the end of mitosis when decreasing phosphorylation is occurring (with regard to rates and differences).

Third, the ratio of intensities, M to G2, for each of the lines differs and the intensity of pS780 and MPM-2 does not correlate between cell lines. Therefore, the antigen density and/or the net activity of the responsible enzyme systems varies between cell lines. This variation is not enough to eliminate the use of the pS780 as a mitotic marker.

Fourth, the detection of mitotic cells in DU-145 cells that do not express appreciable Rb was robust and efficient using the phospho-S780-Rb antibody. Therefore, pS780 resides on proteins in addition to Rb.

Multiple Proteins are Recognized by Antibody to Phospho-S780-Rb

To examine specificity of the phospho-S780 antibody at the peptide level, we performed western blots on lysates of several human cell lines that were untreated or treated with nocodazole (Fig. 6). In these experiments, a band at 140 kDa and a cluster of bands from 57 to 63 kDa increased upon nocodazole treatment. A band that migrated at 103 kDa that was consistent with Rb (confirmed by immunoblotting with antibody to Rb) increased in several experiments (e.g., Fig. 6A) but not all (e.g., Fig. 6B). Further, bands were detected that migrated at the same mobility as Rb but were clearly not Rb (Fig. 6B, SAOS-2) and also did not increase with nocodazole treatment. Flow cytometry of SAOS-2 cells stained with phospho-S780-Rb and MPM2 showed robust detection of mitotic cells (Fig. 6C). SAOS-2 cells, like DU-145, poorly express a truncated unstable protein (33). These data further support the idea that the pS780 epitope resides on several proteins; that it is present in interphase cells as well as mitotic cells, and that the reactivity for some proteins increased in mitosis.⁵ Further, these data suggest that Rb is phos-

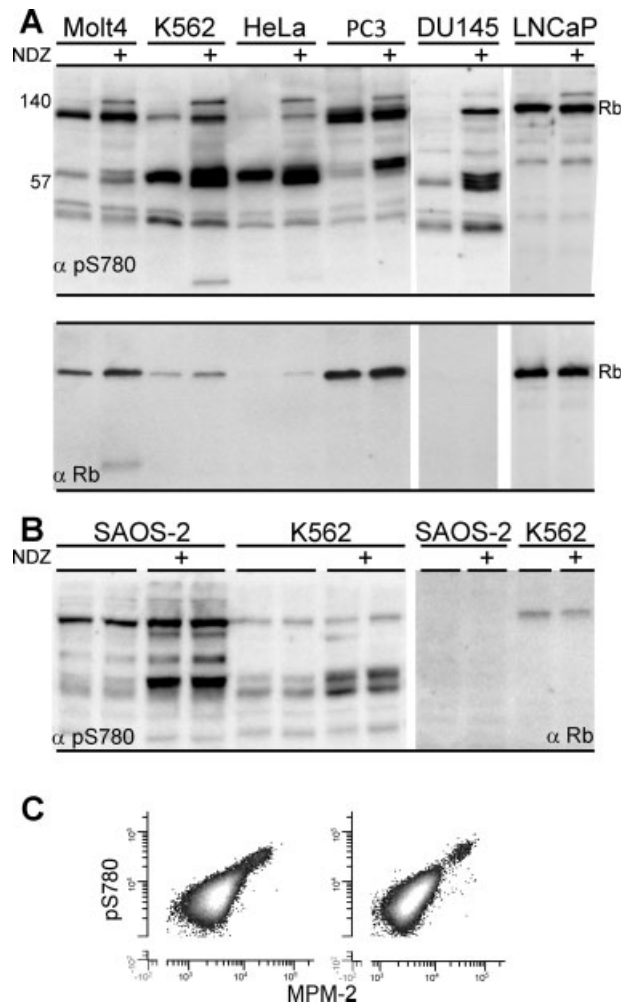


Figure 6. Phospho-S780-Rb recognizes peptides in addition to Rb. (A) Immunoblots for several cell lines including DU-145, which poorly express Rb with an exon 21 deletion. NDZ = nocodazole treatment for 17 h. (B) Immunoblot of SAOS-2 cells that poorly express a truncated Rb. K562 cells are an Rb positive control. The α -pS780 lanes are in duplicate. (C) Bivariate histograms of pS780 and MPM-2 for Rb-positive Molt4 (left) and Rb-negative SAOS-2 (right) cells showing mitotic cell detection by immunoreactivity of phospho-S780-Rb antibody in Rb positive and negative cell lines. (Antibodies (α) for each immunoblot are labeled on the blots.)

phorylated in mitosis at this site but not necessarily at an increased fraction of total Rb. Detection of Rb phosphorylation in mitosis is affected by the presence of reactive bands that appear not to undergo increased mitotic phosphorylation but migrate the same as Rb. Also, the level of Rb protein increases throughout the cell cycle and the increase in phospho-S780-Rb reactivity is similar to the increase in total Rb reactivity (calculated for some experiments from immunoblots of untreated and nocodazole treated samples). We also immunoprecipitated peptides from SAOS-2 and K562 cells with phospho-S780-Rb. Rb was immunoprecipitated from K562 but not SAOS-2 cells (Supplemental Fig. 1). We also performed a western blot on the immunoprecipitates with MPM-2. Very few MPM-2 positive peptides were immunoprecipitated by phospho-S780-Rb; how-

⁴M to G1 transition cells that are not resolved by the pS780-MPM-2 plots in Figure 5 but are readily apparent in the MPM-2/Cyclin A plots are also present.

⁵These data do not distinguish between increased phosphorylation, increased protein content, or both. However, increased phosphorylation is more likely.

ever, an MPM-2 positive peptide that migrated at the molecular mass of Rb was detected in K562 and not in SAOS-2 cells (Supplemental Fig. 1).

Bands at 57 and 140 kDa are Phosphorylated Peptides

A membrane with transferred peptides from nocodazole treated cells was divided in two and treated with calf alkaline phosphatase (CAP) or phosphatase buffer before immunostaining for pS780. Figure 7 shows that the bands at 140 kDa and 57 kDa disappeared, and therefore, are phosphorylated epitopes. The prominent bands at 63 kDa decreased upon CAP treatment and, therefore, are likely to be phosphopeptides. The case for phosphorylation of all the bands that migrate with Rb is less clear. This result was obtained twice. To confirm further, we treated Molt4 and K562 cells with okadaic acid at a concentration that inhibits protein phosphatase 2A (34,35) and subjected lysates to western blotting for pS780. The immunoreactivity of both the 140 kDa and 57–63 kDa bands increased significantly in the OA treated samples (Supplemental Fig. 2).

The pS780 Epitope Reactivity Remains after Acid Denaturation of DNA

Beyond simple counting of mitotic cells and phase fraction analysis, cytometry can be used for complex cell cycle analysis (36). An analysis that we use often is BrdU labeling to obtain timing information (37,38). Combining a mitotic marker, DNA content, and cyclin A can be a powerful combination for measuring the G2 → M → G1 transitions (22). Although there are other approaches, in our hands, acid denaturation of DNA is the most reliable and general of the methods for detecting BrdU incorporation. To combine two or more immunofluorescence probes (e.g., cyclin A, BrdU, and a mitotic marker) in which all probes are mouse monoclonal antibodies requires primary labeled antibodies or antibodies of different heavy chain classes and isotype specific secondary antibodies. We have found it convenient to use different combinations of primary and secondary labeling. In this regard, the use of rabbit antibodies to phospho-S10-histone H3 as a mitotic marker and secondary staining has been especially useful because the secondary antibody fluorochrome could be chosen as needed. For example, we have used secondaries labeled with Pacific Blue, Pacific Orange, and Alexa

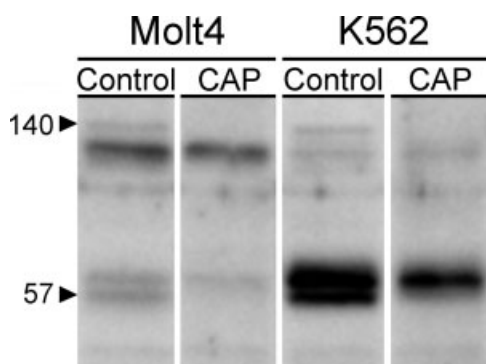


Figure 7. The pS780 epitope is a phospho-epitope. Western blots with phospho-S780-Rb antibody with and without treatment of the membrane with calf alkaline phosphatase are shown.

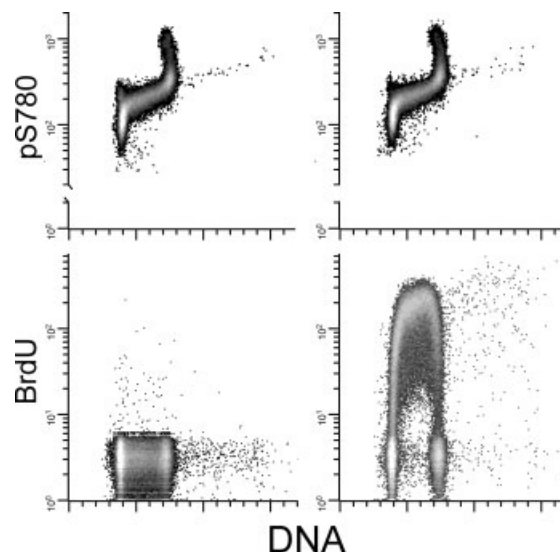


Figure 8. The pS780 epitope is resistant to acid treatment. Bivariate histograms of pS780 versus DNA content or anti-BrdU fluorescence for Molt4 cells are shown. Left panels are from the control (no BrdU incorporation, acid treatment). Right panels are from cells labeled for 30 min. Compare top two panels to Figure 1 (bottom left panel).

700 to enable analyses in which FITC, phycoerythrin, and Alexa 647 have been used on other probes. A problem with phospho-S10-histone H3 as a mitotic marker in BrdU studies is that histones are extracted by acid treatment. Therefore, we tested the pS780 epitope for stability to acid denaturation. Figure 8 shows bivariate plots of pS780 versus DNA with and without BrdU labeling (top panels). Bivariate histograms of BrdU immunofluorescence versus DNA for the same samples are shown in the bottom panels. Detection of mitotic cells is as robust in these samples as in samples that are not treated with acid (e.g., Fig. 1).

To demonstrate further the utility in BrdU labeling, we performed a kinetic analysis of exponentially growing Molt4 after 30 min labeling with BrdU. The cells were labeled, then chased with thymidine, and thereafter sampled at time intervals and fixed for later staining with antibodies to cyclin A, pS780, and BrdU, and DAPI. The primary gating strategy is shown in supplemental data Figure 3. The secondary gating strategy is shown in Figure 9A. After gating on singlets and live cells,⁶ mitotic cells (color coded blue), and G2 cells (color coded green), the bivariate distribution of cyclin A and pS780 was used to set up regions of interest (Fig. 9A). In this plot, the regions R6 and R7 are sequential (early → late) windows on G2.⁷ R8 is a window in the intermediate region that can be classified as early prophase, late G2, or in between based on available information. It is the period during which the enzymes that result in phosphorylation of the pS780 epitope (net activity of kinases and phosphatases) are changing such that phosphorylation is between bistable states. R9 through R11 are sequential regions through mitosis. R9 is consistent with prophase cells (high levels of cyclin

⁶That is, cells that were alive at the time of fixation.

⁷See supplemental Figure 3 and its legend for explanation of G2 analytical definition.

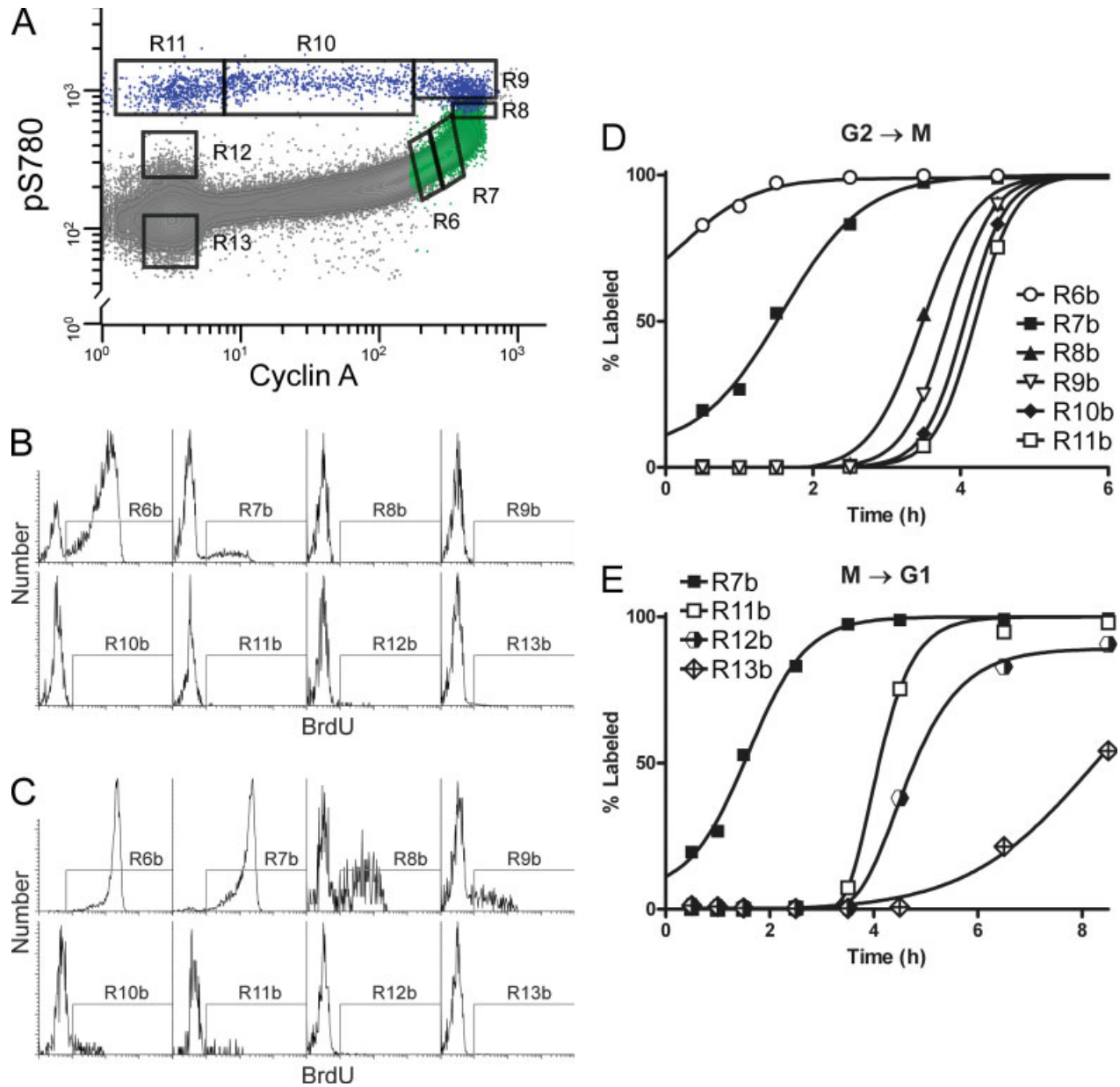


Figure 9. Gating scheme for kinetic analysis of the G2 → M → G1 transition. The top panel (A) shows a pS780 versus cyclin A bivariate histogram for BrdU labeled Molt4 cells at $t = 0.5$ h (immediately after labeling for 30 min). The cells represented in this plot were from the 2C stem line only (i.e., the 4C endoreduplicated cells have been gated out). Color coding: G2 = green, M = blue, gray = all the rest. The complete gating scheme is described in detail in Supplemental Figure 3. Gates were set on the upper panel histogram to delimit the approximate first and second tertiles of the bivariate G2 distribution (R6, R7); the transition-phase (between G2 and M) (R8); prophase cells (R9); prometaphase cells (R10); and late mitosis (R11). Additional gates were set on a pS780 positive G1 “nub” (R12) and the lower half of the main cluster of G1 cells (R13) (identified additionally by DNA content). The second and third panels (B and C) are the BrdU distributions at $t = 0.5$ h (B) and $t = 3.5$ h (C) with each panel (moving left to right) representing the cells gated from R6 through R13 (R6b maps to R6, etc.). Note the change in positive cell numbers in the first 6 panels from 0.5 to 3.5 h. D and E show the fraction of labeled cells plotted versus time for each of the panels depicted in B and C (R6b through R13b are the positive gates mapping to R6 through R13). Panel D shows the relevant curves that are used to calculate transit times for the G2 to M transitions. Panel E shows the same curves covering the M to G1 transition.

A). R10 is consistent with prometaphase (cyclin A levels are intermediate and in the process of decreasing). R11 is consistent with metaphase through telophase and cytokinesis (cyclin A is depleted to the levels associated with absence of mitotic cyclins (the anti-mitotic window governed by Cdh1)). R12 is a region set on a nub of hyper reactivity of pS780 in G1 (defined by ab-

sence of cyclin A and 2C DNA content). R13 is set on G1 cells that have levels of pS780 below the median reactivity for all G1. The precedence that we expected was R6 → R12. Figures 9B and 9C show the resulting single parameter BrdU immunofluorescence histograms at $t = 0.5$ and 3.5 h with each panel and: “Rxb” corresponding to Rx gates/regions in 9A with additional

Table 2. Cells tested

LYMPHOID	MYELOID	EPITHELIAL	FIBROBLAST
T cells	K562	Hela	hTert-BJ1
Molt4		PC3	
		DU145	
		22Rv1	
		hTert-RPE-1	
		RKO	

gates to ensure that only the 2C stemline was analyzed (as shown in Supplemental data).

The percentage of positive labeled cells at each time point for each region (R6b through R13b) are plotted in Figures 9D and 9E. As expected, the labeled cells “pass through” the windows R6 through R12 sequentially. Note that the slope of the curves used to fit the data, are sharper for the mitotic windows than for the G2 or G1 windows, as expected for the reduction of variation as the cell cycle progresses. Also, note that the time delay at the half-max points between the “newborn” nub (R12) and the region set on the bottom half of the pS780 epitope G1 distribution (R13) is long enough to guess that the pS780 distribution in G1 is not informative with respect to time—that is, it is not likely that G1 cells are appreciably younger or older at different levels pS780 (with the exception of the “nub”). Therefore, there are two states in G1 with respect to the pS780 epitope—“newborn” cells that are post-cytokinetic and all the rest. This means that cells start out in the “newborn” nub then descend (lose the mitotic phosphorylation) and then start the interphase cycle again from some random point within the large G1 cluster. This may not apply in the situation where a true G0 state exists, since activated G1 lymphocytes can easily be distinguished from resting lymphocytes (Supplemental Fig. 4). A final note to make about these data is that very short time periods along the cell cycle can be measured effectively. Subtracting the halftimes of the curves for R9b–R8b, R10b–R9b, and R11b–R10b gives values of 21.2, 13.6, and 8.2 min, respectively. Adding these together, the median early mitosis length was 42 min (from the onset of pS780 mitotic phosphorylation to metaphase).

The pS780 Mitotic Pattern is Ubiquitous

Every cell line or cell type that we have tested has rendered an immunofluorescence versus DNA pattern that identifies mitotic cells. Table 2 lists the cell lines we have tested. Most are human solid tumor or hematopoietic cancer cell lines. The hTert lines are immortal, non-tumorigenic, euploid human cell lines. We have also tested stimulated human T cells. Data demonstrating this for T cells are presented in Supplemental Figure 4.

Nature of the pS780 Epitope

We have presented significant evidence that the antibody phospho-S780-Rb recognizes an epitope or closely related epitopes on several peptides with high affinity. These are phosphopeptides and are highly expressed in mitosis. This expression is likely to be due to elevated kinase activity since it is

highly correlated with MPM-2 epitope expression. Although reactivity with the two antibodies is highly correlated on a cellular basis, there is little overlap in terms of the peptides on which the epitopes are expressed. Like MPM-2, pS780 is resistant to the acid treatment used to stain cells for BrdU. Thus, pS780 is a robust marker for mitosis and useful as an alternative to MPM-2 in complex cytometric analysis of the cell cycle. We searched the human genome for translated sequences that might constitute the core of the epitope. As a start toward identifying the epitope, we limited the search to peptides of predicted mass of 130–150 kDa; at least one serine residue, and at least four contiguous amino acids contained within the sequence PTLSPIPH. That search produced 18 peptides (due to isoforms) and 13 genes that code TLSP; 8 peptides that code SPIP; 6 peptides (5 genes) that code PTLs, and 3 peptides (2 genes) that code LSPI. This suggests that using informatics as a guide and synthetic peptide inhibition, we may be able to identify the epitope.

ACKNOWLEDGEMENTS

We wish to thank Minh Lam for assistance with confocal microscopy. We thank Randy Wetzel and Brad Smith (Cell Signaling Technology, Danvers, MA) for generous gifts of phospho-S780-Rb antibody and SOAS-2 cells; T. Vincent Shankey for the generous gift of PE conjugated cyclin A antibody, and Ed Luther (Compucyte Inc., Cambridge, MA) for the algorithm to identify mitotic cells by LSC.

LITERATURE CITED

- Anderson HJ, de Jong G, Vincent I, Roberge M. Flow cytometry of mitotic cells. *Exp Cell Res* 1998;238:498–502.
- Juan G, Traganos F, James WM, Ray JM, Roberge M, Sauve DM, Anderson H, Darzynkiewicz Z. Histone H3 phosphorylation and expression of cyclins A and B1 measured in individual cells during their progression through G2 and mitosis. *Cytometry* 1998;32:71–77.
- Clevenger CV, Epstein AL, Bauer KD. Modulation of the nuclear antigen p105 as a function of cell-cycle progression. *J Cell Physiol* 1987;130:336–343.
- Andreassen PR, Margolis RL. Microtubule dependency of p34cdc2 inactivation and mitotic exit in mammalian cells. *J Cell Biol* 1994;127:789–802.
- Gong J, Traganos F, Darzynkiewicz Z. Discrimination of G2 and mitotic cells by flow cytometry based on different expression of cyclins A and B1. *Exp Cell Res* 1995; 220:226–231.
- Di Vinci A, Geido E, Pfeffer U, Vidali G, Giaretti W. Quantitative analysis of mitotic and early-G1 cells using monoclonal antibodies against the AF-2 protein. *Cytometry* 1993;14:421–427.
- Nolan GP. Deeper insights into hematological oncology disorders via single-cell phospho-signaling analysis. *Hematology Am Soc Hematol Educ Program* 2006; 509:123–127.
- Perez OD, Nolan GP. Phospho-proteomic immune analysis by flow cytometry: From mechanism to translational medicine at the single-cell level. *Immunol Rev* 2006; 210:208–228.
- Hedley DW, Chow S, Goolsby CL, Shankey TV. Pharmacodynamic monitoring of molecular-targeted agents in the peripheral blood of leukemia patients using flow cytometry. *Toxicologic Pathology* (in press).
- Jacobberger JW, Sramkoski RM, Zhang D, Zumstein LA, Doerksen LD, Merritt JA, Wright SA, Shults KE. Bivariate analysis of the p53 pathway to evaluate Ad-p53 gene therapy efficacy. *Cytometry* 1999;38:201–213.
- Monier K, Mouradian S, Sullivan KF. DNA methylation promotes Aurora-B-driven phosphorylation of histone H3 in chromosomal subdomains. *J Cell Sci* 2007;120: 101–114.
- Scrittore L, Skoufias DA, Hans F, Gerson V, Sassone-Corsi P, Dimitrov S, Margolis RL. A small C-terminal sequence of Aurora B is responsible for localization and function. *Mol Biol Cell* 2005;16:292–305.
- Crosio C, Fimia GM, Loury R, Kimura M, Okano Y, Zhou H, Sen S, Allis CD, Sassone-Corsi P. Mitotic phosphorylation of histone H3: spatio-temporal regulation by mammalian Aurora kinases. *Mol Cell Biol* 2002;22:874–885.
- Wang R, He G, Nelman-Gonzalez M, Ashorn CL, Gallick GE, Stukenberg PT, Kirschner MW, Kuang J. Regulation of Cdc25C by ERK-MAP kinases during the G2/M transition. *Cell* 2007;128:1119–1132.

15. Escargueil AE, Larsen AK. Mitosis-specific MPM-2 phosphorylation of DNA topoisomerase II α is regulated directly by protein phosphatase 2A. *Biochem J* 2007;403:235–242.
16. Andreassen PR, Skoufias DA, Margolis RL. Analysis of the spindle-assembly checkpoint in HeLa cells. *Methods Mol Biol* 2004;281:213–225.
17. Mahnke YD, Roederer M. Optimizing a multicolor immunophenotyping assay. *Clin Lab Med* 2007;27:469–485.
18. Geng Y, Yu Q, Sicinska E, Das M, Bronson RT, Sicinski P. Deletion of the p27Kip1 gene restores normal development in cyclin D1-deficient mice. *Proc Natl Acad Sci USA* 2001;98:194–199.
19. Kitagawa M, Higashi H, Jung HK, Suzuki-Takahashi I, Ikeda M, Tamai K, Kato J, Segawa K, Yoshida E, Nishimura S, Taya Y. The consensus motif for phosphorylation by cyclin D1-Cdk4 is different from that for phosphorylation by cyclin A/E-Cdk2. *Embo J* 1996;15:7060–7069.
20. Sramkoski RM, Pretlow TG II, Giaconia JM, Pretlow TP, Schwartz S, Sy MS, Marengo SR, Rhim JS, Zhang D, Jacobberger JW. A new human prostate carcinoma cell line, 22Rv1. *In Vitro Cell Dev Biol Anim* 1999;35:403–409.
21. Jacobberger JW, Sramkoski RM, Frisa PS, Ye PP, Gottlieb MA, Hedley DW, Shankey TV, Smith BL, Paniagua M, Goolsby CL. Immunoreactivity of Stat5 phosphorylated on tyrosine as a cell-based measure of Bcr/Abl kinase activity. *Cytometry A* 2003;54A:75–88.
22. Soni DV, Jacobberger JW. Inhibition of cdk1 by alsterpaullone and thioflavopiridol correlates with increased transit time from mid G2 through prophase. *Cell Cycle* 2004;3:349–357.
23. Jacobberger JW, Fogleman D, Lehman JM. Analysis of intracellular antigens by flow cytometry. *Cytometry* 1986;7:356–364.
24. Schimenti KJ, Jacobberger JW. Fixation of mammalian cells for flow cytometric evaluation of DNA content and nuclear immunofluorescence. *Cytometry* 1992;13:48–59.
25. Sramkoski RM, Wormsley SW, Bolton WE, Crumpler DC, Jacobberger JW. Simultaneous detection of cyclin B1, p105, and DNA content provides complete cell cycle phase fraction analysis of cells that endoreduplicate. *Cytometry* 1999;35:274–283.
26. Jacobberger JW. Stoichiometry of immunocytochemical staining reactions. *Methods Cell Biol* 2001;63:271–298.
27. Frisa PS, Lanford RE, Jacobberger JW. Molecular quantification of cell cycle-related gene expression at the protein level. *Cytometry* 2000;39:79–89.
28. Kametsky LA, Kametsky LD. Microscope-based multiparameter laser scanning cytometer yielding data comparable to flow cytometry data. *Cytometry* 1991;12:381–387.
29. Bodnar AG, Ouellette M, Frolkis M, Holt SE, Chiu CP, Morin GB, Harley CB, Shay JW, Lichtsteiner S, Wright WE. Extension of life-span by introduction of telomerase into normal human cells. *Science* 1998;279:349–352.
30. Che S, Weil MM, Nelman-Gonzalez M, Ashorn CL, Kuang J. MPM-2 epitope sequence is not sufficient for recognition and phosphorylation by ME kinase-H. *FEBS Lett* 1997;413:417–423.
31. Wang X, Deng H, Basu I, Zhu L. Induction of androgen receptor-dependent apoptosis in prostate cancer cells by the retinoblastoma protein. *Cancer Res* 2004;64:1377–1385.
32. den Elzen N, Pines J. Cyclin A is destroyed in prometaphase and can delay chromosome alignment and anaphase. *J Cell Biol* 2001;153:121–136.
33. Shew JY, Lin BT, Chen PL, Tseng BY, Yang-Feng TL, Lee WH. C-terminal truncation of the retinoblastoma gene product leads to functional inactivation. *Proc Natl Acad Sci USA* 1990;87:6–10.
34. Favre B, Turowski P, Hemmings BA. Differential inhibition and posttranslational modification of protein phosphatase 1 and 2A in MCF7 cells treated with calyculin-A, okadaic acid, and tautomycin. *J Biol Chem* 1997;272:13856–13863.
35. Millward TA, Zolnierowicz S, Hemmings BA. Regulation of protein kinase cascades by protein phosphatase 2A. *Trends Biochem Sci* 1999;24:186–191.
36. Darzynkiewicz Z, Crissman H, Jacobberger JW. Cytometry of the cell cycle: Cycling through history. *Cytometry A* 2004;58A:21–32.
37. Begg AC, McNally NJ, Shrieve DC, Karcher H. A method to measure the duration of DNA synthesis and the potential doubling time from a single sample. *Cytometry* 1985;6:620–626.
38. White RA, Terry NH. A quantitative method for evaluating bivariate flow cytometric data obtained using monoclonal antibodies to bromodeoxyuridine. *Cytometry* 1992;13:490–495.
39. Gasnereau I, Ganier O, Bourgain F, de Gramont A, Gendron MC, Sobczak-Thépot J. Flow cytometry to sort mammalian cells in cytokinesis. *Cytometry A* 2007;71A:1–7.